

A Real-Time Tea Leaf Disease Detection System for Tea Leaves Based on YOLOv10 and a Customized Handheld Terminal

Xiao Li, Bin Yang, Jiayi Luo, Guixiu Xie, Xiaoliang Liang, Jiaxue Li*

Guangdong Technology College, Zhaoqing, 526100, Guangdong Province, China

*Corresponding author

Abstract: Early detection and precise management of tea leaf diseases and pests are essential for maintaining tea yield and quality. In China, the average annual loss attributed to tea leaf diseases and pests is approximately 15%-20%. Conventional manual inspection is costly, time-consuming, and poorly suited to rapid early warning under complex tea plantation conditions. To address these limitations, this study proposes and implements a real-time tea leaf disease detection system that integrates YOLOv10 with a customized handheld terminal. For hardware-based data acquisition, a utility-model-patented touch-controlled handheld imaging terminal was developed. The terminal incorporates a rotary stage and an anti-slip spring-seat mechanism, which effectively suppresses device shake during one-handed field operation and improves the stability of image acquisition. For algorithmic recognition, an efficient YOLOv10 object detector with a non-maximum suppression (NMS)-free design is introduced and deployed on an edge computing node. Experimental results on a test set containing healthy leaves and seven representative diseases (algal leaf disease, anthracnose, bird's-eye spot, brown blight, gray spot disease, red leaf spot disease, and white spot disease) show that the proposed system achieves an overall mean average precision (mAP@0.5) of 0.753. In particular, the recognition precision for visually distinctive diseases such as red leaf spot disease (redleafspot) reaches 0.950. The system also achieves an inference speed of 150 FPS, satisfying the low-latency requirements of real-time detection. By coupling customized hardware with a lightweight deep learning model, the proposed system reduces detection cost and response time, providing a practical engineering solution for disease monitoring and automation in smart tea plantations.

Keywords: smart agriculture; tea leaf disease detection; YOLOv10; object detection

1. Introduction

Tea is a major agricultural commodity worldwide and plays an important role in the economic development and international trade of many countries. China is one of the world's leading tea producers and exporters, and the tea industry makes a substantial contribution to the national economy. During tea growth, however, plants are vulnerable to a range of diseases and pests, including anthracnose, brown blight, and red leaf spot disease. Statistics indicate that China's tea planting area exceeds 45 million mu, and the average annual loss caused by diseases and pests is approximately 15%-20%. Because early symptoms of tea leaf infection are often inconspicuous, conventional visual observation cannot reliably determine whether infection has occurred, which may delay intervention and lead to large-scale spread. Therefore, early, rapid, and accurate detection of tea leaf diseases is critical not only for improving tea quality and farmers' income, but also for advancing green prevention and control technologies in ecological tea plantations. Current domestic studies on tea leaf disease detection still rely largely on conventional methods, including manual observation, microscopic examination, and biochemical analysis. Manual observation is strongly dependent on the subjective experience of technicians and is difficult to apply to large-scale rapid detection. Targeted control of brown leaf spot disease provides a practical disease-management reference for tea plantations [1]. Tea leaf state recognition based on deep learning further indicates that visual features can support field diagnosis [2]. Studies on improving tea output value highlight the economic motivation for disease monitoring [3]. Tea plucking and management research clarifies the production context in which field detection systems are deployed [4]. Microscopic examination requires complex sample preparation, such as sectioning and staining, and is labor-intensive and time-consuming. Although biochemical analysis can achieve accurate molecular-level detection, its long detection cycle and high cost make it unsuitable for the rapid

circulation requirements of tea production and trade. In recent years, artificial intelligence technologies represented by deep learning have shown considerable promise in agricultural disease detection. YOLOv10 provides a real-time end-to-end detection framework for low-latency object recognition [5]. GDE-YOLO demonstrates that tea leaf diseases can be detected in complex plantation environments [6]. Recent deep-learning algorithms for tea disease detection further support the feasibility of model-based diagnosis [7]. Comparative studies of VGG16, Vision Transformer, EfficientNetB3, and Xception show that different deep architectures can be adapted to tea leaf disease classification [8]. Computer vision research in tea production summarizes the broader application basis for intelligent tea-field monitoring [9]. CNN-based region proposal methods provide a reference for plant disease image identification [10]. YOLOX shows the continuing evolution of YOLO-series detectors and their efficiency-oriented design [11]. Crop disease image recognition research based on deep learning provides methodological support for transferring visual detection models to agricultural scenarios [12]. For example, Washington State University in the United States developed an apple disease detection system based on convolutional neural networks (CNNs), and European research teams have combined unmanned aerial vehicles with multispectral sensors for rapid monitoring of crop diseases. Nevertheless, most agricultural AI enterprises focus on field crops such as rice and wheat, whereas applications in the tea domain remain at an early stage with few competing solutions. Computer-vision-based rice variety recognition illustrates the use of visual features in crop identification [13]. Computer vision has also been applied to log-volume measurement, showing its value in non-contact measurement tasks [14]. Reviews of convolutional neural networks in visual image detection provide a general algorithmic basis for this study [15]. In addition, directly applying computer vision to complex, unstructured tea plantation environments faces a serious hardware deployment constraint: conventional handheld devices are prone to shake during one-handed field operation, producing blurred images and substantially reducing the recognition accuracy of downstream object detection algorithms. To address these industrial needs and technical bottlenecks, this paper proposes and implements a real-time tea leaf disease detection and recognition system based on the collaboration between the YOLOv10 algorithm and patented hardware. Tea-bud detection and leaf-disease image recognition based on deep learning support the integration of tea-specific visual perception with field acquisition hardware [16]. Computer-vision-based recognition and localization of high-quality tea buds further supports the hardware-oriented deployment scenario considered in this paper [17]. The main contributions are as follows:

Customized hardware innovation: A touch-controlled handheld imaging terminal was designed and developed. The terminal introduces an anti-slip gripping mechanism consisting of a base platform, a rotary stage, a spring-driven component, and a slide plate. This mechanical structure compensates for instability during one-handed field operation and improves input image clarity at the hardware level.

Efficient lightweight algorithm deployment: An NMS-free YOLOv10 algorithm is introduced into the vertical task of tea leaf disease detection. Compared with conventional large-scale CNN models, YOLOv10 maintains detection accuracy while achieving an inference speed of up to 150 FPS, making it suitable for low-cost edge devices with limited computing resources.

Comprehensive engineering validation: The system was evaluated on a high-quality dataset containing healthy leaves and seven representative diseases. The results show that the system can detect multiple disease targets simultaneously and achieves an overall mean average precision (mAP@0.5) of 0.753, thereby reducing dependence on specialized laboratory equipment and complicated sample preparation.

2. System Hardware Design and Data Acquisition

High-quality image input is a prerequisite for stable operation of deep learning-based computer vision systems. In complex and unstructured tea plantation environments, terrain undulation and operator movement can readily induce mechanical vibration in acquisition devices. Therefore, this study designs an image acquisition and control architecture that combines a customized handheld terminal with unmanned aerial vehicle collaboration, thereby improving data clarity and reliability at the physical hardware level.

2.1. Dual-Modal Image Acquisition and Preprocessing Strategy

The system adopts a data acquisition strategy that combines macroscopic and microscopic observations. At the macroscopic level, unmanned aerial vehicles are used to perform comprehensive multi-angle coverage flights over large tea plantation areas. At the microscopic level, a high-resolution

color line-scan camera and the touch-controlled handheld imaging terminal are used to capture fine-grained features at close range.

After optical image signals are obtained, the system converts them into electrical signals for pre-amplification and processing. To satisfy the input dimensionality and feature extraction requirements of YOLOv10, the front end of the system integrates an automated image preprocessing module that performs spatial alignment operations such as cropping, rotation, and scaling (Fig. 1). A binarization mechanism is also introduced to enhance image contrast, separate disease features from complex backgrounds, and maintain color fidelity and resolution.

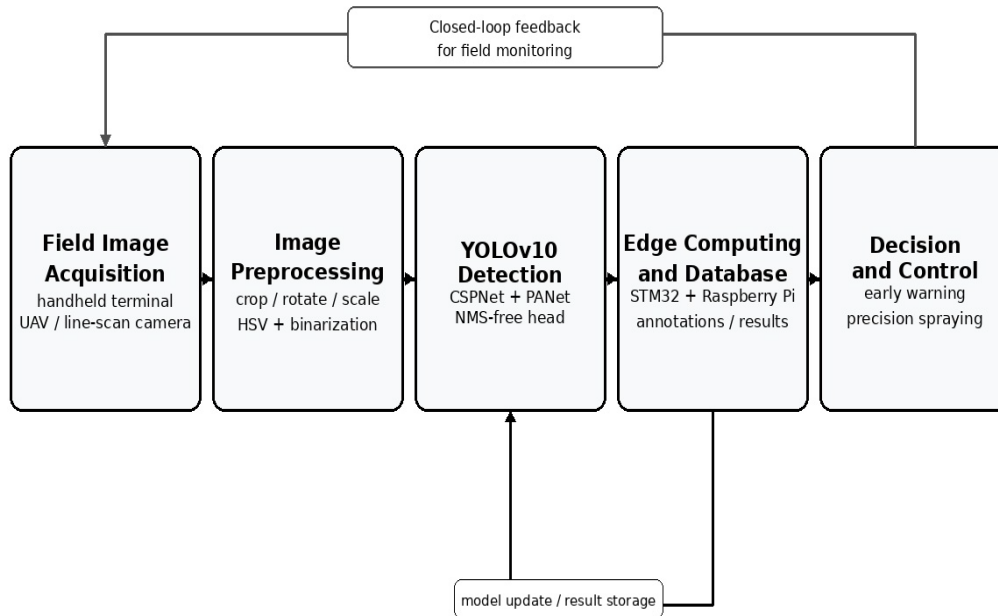
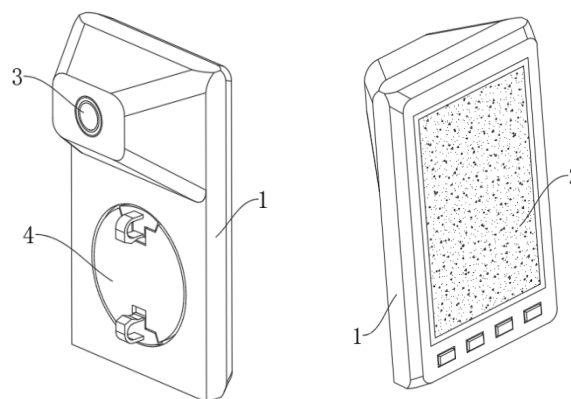


Fig. 1 Overall Architecture Diagram of Distributed Image Acquisition and Edge Control System for Smart Tea Plantation

2.2. Mechanical Structure Optimization of the Touch-Controlled Handheld Imaging Terminal

To address device shake during one-handed field operation, a customized touch-controlled handheld imaging terminal was developed (Fig.2). The terminal was optimized in terms of human-computer interaction and physical vibration suppression.



1. Main body 2. Touch screen 3. Camera module 4. Grip plate

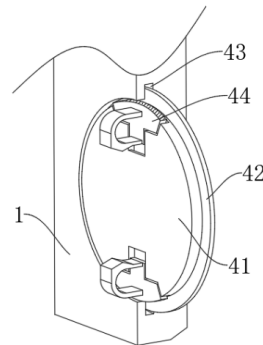
Fig. 2 Structural Diagram of the Touch-Controlled Handheld Imaging Terminal

2.2.1. Terminal Body and Rotary Attitude Adjustment Mechanism

The main structure of the device includes a body, a front touch screen, and a high-definition camera module mounted on the upper rear side (Fig.3). To improve the convenience and flexibility of one-handed operation, a dedicated grip plate is arranged below the camera module on the rear side of

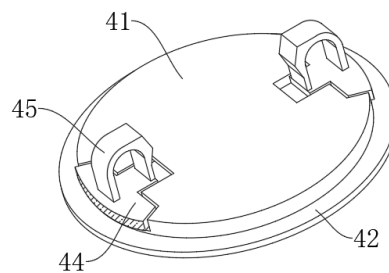
the body (Fig.4).

To enable flexible framing in complex fields of view, a rotation cavity is arranged on the rear side of the body. The core base platform of the grip plate is fitted into the rotation cavity through a rotary stage, forming a rotational connection between the base platform and the body. This mechanism allows the user to swing and adjust the angle of the body during gripping without changing wrist posture, thereby enabling more stable tapping and swiping on the front touch screen and more accurate image capture.



1. Main body 41. Base platform 42. Rotary stage 43. Rotation cavity 44. Anti-slip seat

Fig. 3 Rear View of the Touch-Controlled Handheld Imaging Terminal



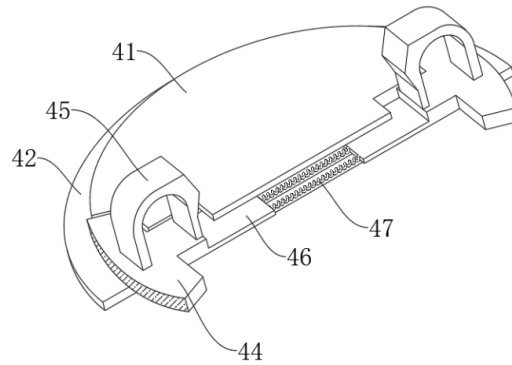
41. Base platform 42. Rotary stage 44. Anti-slip seat 45. Grip handle

Fig. 4 Structural Diagram of the Grip Plate in the Touch-Controlled Handheld Imaging Terminal

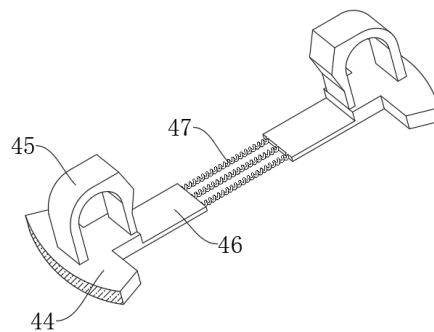
2.2.2. Spring Damping and Anti-Slip Limiting Mechanism

To stabilize the adjusted posture and prevent slippage at the moment of image capture, a mechanical anti-slip structure is integrated into the grip plate.

The mechanism consists of an anti-slip seat, a grip handle, a slide plate, and a driving component (spring) (Fig.5 and 6). A slide plate is formed at the lower end of the anti-slip seat, inserted into the grip plate, and maintained in a sliding connection. In the natural state, the internal spring acts as the driving component and presses the slide plate, forcing the anti-slip seat to contact the body tightly and generating sufficient friction for anti-slip limiting. When the operator needs to adjust the imaging angle, toggling the grip handle drives the slide plate to compress the spring, separates the anti-slip seat from the body, and releases the limit lock. After adjustment, releasing the grip handle allows the restoring force of the spring to return the anti-slip seat immediately to the contact state and re-lock the body. This spring-damping-based physical vibration suppression design improves image quality during real-time field sampling.



41. Base platform 42. Rotary stage 44. Anti-slip seat 45. Grip handle 46. Slide plate 47. Spring
Fig. 5 Sectional View of the Connection between the Body and Grip Plate in the Touch-Controlled Handheld Imaging Terminal



44. Anti-slip seat 45. Grip handle 46. Slide plate 47. Spring

Fig. 6 Sectional View of the Grip Plate Structure in the Touch-Controlled Handheld Imaging Terminal

2.3. Low-Level Hardware Communication and Distributed Control

At the edge computing and communication layer, the system mainboard adopts embedded microcontroller architectures such as STM32 and Raspberry Pi, and a dedicated PCB circuit is designed to ensure reliable execution of low-level hardware logic.

For distributed networking, the system establishes a wireless communication link based on GPRS/CDMA protocols. Data collected by field instrument acquisition stations and PLC acquisition stations in the tea plantation are aggregated through the wireless network and substation switches to the main acquisition server on the public network. This distributed architecture supports low-latency transmission of highly concurrent image data and converts disease recognition results produced by YOLOv10 into control commands, enabling remote automatic spraying devices and other agricultural machinery to perform precise prevention and control.

3. YOLOv10-Based Real-Time Tea Leaf Disease Perception and Feature Extraction Algorithm

After high-resolution field images of tea leaves are acquired, the central algorithmic challenge is to achieve accurate and ultra-low-latency disease detection under the limited computing resources of edge devices. Considering the diverse lesion morphologies, large scale variations, and interference from complex natural backgrounds, this study introduces and adapts the new-generation object detection framework YOLOv10 to construct an end-to-end disease recognition model.

3.1. Image Preprocessing and Feature Enhancement Mechanism

Raw images acquired by unmanned aerial vehicles and handheld terminals usually contain substantial non-target regions, such as soil and trunks, as well as shadows caused by uneven illumination (Fig.7). To enhance the sensitivity of YOLOv10 to disease features, an automated

preprocessing pipeline is designed at the feature input stage.



Fig. 7 Effect of Tea Leaf Disease Image Preprocessing and Adaptive Threshold-Based Morphological Separation

3.1.1. Spatial Geometric Alignment and Scale Normalization

To address viewpoint differences between unmanned aerial vehicle top-view imaging and handheld close-range imaging, the preprocessing module first performs spatial geometric alignment on input images. Affine transformations, including cropping, rotation, and translation, are used to correct image tilt, and bilinear interpolation is adopted to resize images uniformly to the standard resolution required by the network, such as 640 X 640. This step reduces scale deviations introduced by different device viewpoints and ensures that the model receptive field accurately covers disease features.

3.1.2. Morphological Separation of Targets and Background

At the early stage of disease development, color differences between lesions and healthy leaf tissue are often subtle. To highlight diseased regions, Adaptive Threshold Binarization is introduced during preprocessing. Images are transformed from the RGB color space to the HSV space, where disease-related features are more distinguishable, and the Hue and Saturation channels that are sensitive to disease symptoms are extracted. Dynamic thresholds are then used to separate disease features from complex tea plantation backgrounds and shadows, thereby improving local contrast and removing substantial redundant noise before feature extraction by the deep neural network.

3.2. YOLOv10 Model Architecture and Adaptation to Tea Leaf Diseases

Conventional YOLO-series algorithms, such as YOLOv5/v8, rely heavily on non-maximum suppression (NMS) during post-processing to remove redundant prediction boxes. This operation increases inference latency and may cause missed detections when lesions overlap or occur densely on tea leaves. The YOLOv10 framework adopted in this study eliminates this bottleneck at the architectural level (Fig.8).

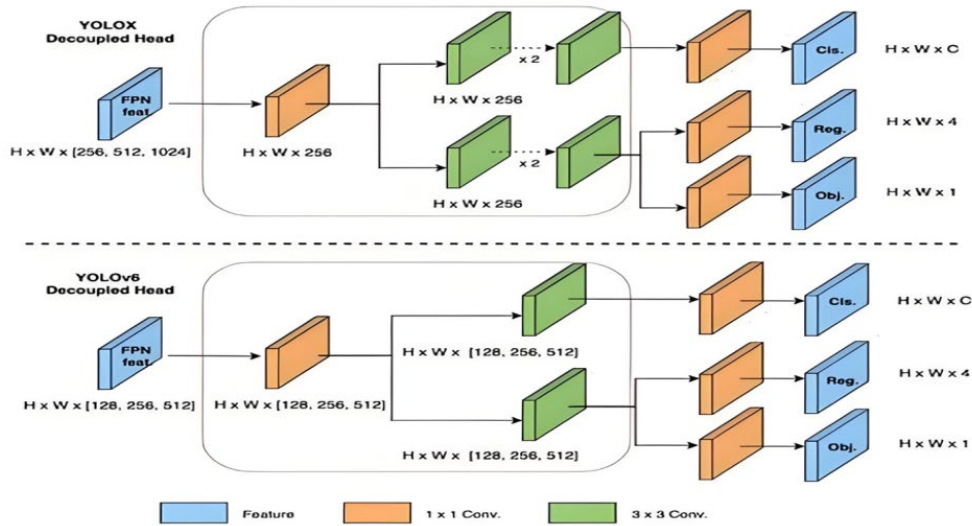


Fig. 8 YOLOv10 Architecture Integrating CSPNet and an NMS-Free Decoupled Head

3.2.1. Multi-Scale Feature Extraction Network

YOLOv10 uses an optimized Cross Stage Partial Network (CSPNet) as the backbone feature extractor. Because tea leaf diseases include both small bird's-eye spot (birdeyespot) lesions and large-area brown blight (brownblight) regions, the neck of the model incorporates a Path Aggregation Network (PANet). This bidirectional feature pyramid, combining top-down and bottom-up information flow, enables sufficient interaction between high-level semantic features and low-level high-resolution spatial features, effectively reducing feature loss for multi-scale lesions.

3.2.2. NMS-Free End-to-End Detection Head

The key algorithmic advantage of this system is the Consistent Dual Assignments strategy. During training, the model simultaneously adopts one-to-many (One-to-Many) and one-to-one (One-to-One) label assignment. During inference, only the one-to-one prediction head is retained. This design removes the NMS post-processing module from the detection pipeline. For agricultural edge devices with limited computing resources, this substantially reduces computational overhead. Experimental results show that, owing to this architecture, the system achieves an end-to-end inference speed of 150 FPS, which satisfies the instantaneous response requirements of real-time disease monitoring and subsequent agricultural machinery, such as linked automatic spraying devices.

3.3. Model Optimization and Multi-Class Joint Training

The detection task in this study covers eight target classes in tea plantation environments: algal leaf disease (algalleaf), anthracnose (Anthracnose), bird's-eye spot (birdeyespot), brown blight (brownblight), gray spot disease (graylight), healthy leaf (healthy), red leaf spot disease (redleafspot), and white spot disease (whitespot). To achieve accurate localization and classification of these targets, the model is optimized during training using a joint loss function L_{total} . The loss function consists of the classification loss L_{cls} and the bounding box regression loss L_{box} :

$$L_{total} = \lambda_1 L_{cls} + \lambda_2 L_{box}$$

where the classification loss L_{cls} is implemented as binary cross-entropy loss (BCE Loss) to distinguish visually similar diseases, such as brown blight and gray spot disease; the bounding box regression loss L_{box} adopts CIoU (Complete Intersection over Union) loss, which jointly considers the overlap area, center-point distance, and aspect-ratio consistency between the predicted and ground-truth boxes. Through multiple rounds of iterative optimization on a large-scale tea leaf dataset, the model learns high-dimensional robust features for distinguishing different disease categories.

4. Experiments and Results Analysis

To comprehensively and objectively evaluate the effectiveness of the proposed tea leaf disease

detection system based on YOLOv10 and customized hardware, this chapter describes the construction of the experimental dataset and the evaluation metrics, and analyzes model performance in terms of class-specific detection accuracy, confusion matrix distribution, and real-time system performance.

4.1. Experimental Dataset and Evaluation Metrics

4.1.1. Dataset Construction and Class Distribution

The dataset in this study was collected at multiple scales in real tea plantation environments using the customized handheld terminal and unmanned aerial vehicles. After data cleaning and expert annotation, a vertical-domain dataset containing eight core tea leaf states was constructed. The eight categories are algal leaf disease (algalleaf), anthracnose (Anthracnose), bird's-eye spot (birdeyespot), brown blight (brownblight), gray spot disease (graylight), healthy leaf (healthy), red leaf spot disease (redleafspot), and white spot disease (whitespot). These categories cover typical pathological phenotypes from healthy tea leaf growth to infection by different pathogens, including fungi, bacteria, and algae.

4.1.2. Evaluation Metrics

To rigorously quantify model perception performance, this paper adopts standard metrics widely used in object detection, including precision (Precision), recall (Recall), and mean average precision (Mean Average Precision, mAP@0.5). In addition, because smart agriculture imposes strict real-time requirements on edge computing systems, frames per second (Frames Per Second, FPS) is included as a system-level evaluation metric.

4.2. Evaluation of Model Detection Accuracy

Inference was performed on the test set to generate Precision-Recall (PR) curves for each category. The area under each PR curve reflects the overall detection capability of the model for the corresponding disease and is expressed as Average Precision (AP).

4.2.1. Overall Detection Performance

The experimental results show that YOLOv10 achieves strong overall recognition performance on the unstructured tea leaf disease dataset, with an overall mean average precision (mAP@0.5) of 0.753. This result indicates that the model can accurately capture lesion features while maintaining robustness in complex scenarios involving multiple overlapping categories.

4.2.2. Class-Specific Performance and Mechanistic Analysis

Detection performance varies across disease categories, mainly because of differences in the visual salience of lesion phenotypes:

High-accuracy recognition group: The model achieves particularly strong recognition performance for red leaf spot disease (redleafspot) and healthy leaf (healthy), with AP values of 0.950 and 0.906, respectively. Red leaf spot disease exhibits strong color contrast against normal green leaves, and healthy leaves show relatively uniform and smooth textures; therefore, the YOLOv10 feature pyramid can effectively extract their highly discriminative semantic features. In addition, anthracnose (Anthracnose) achieves an AP of 0.774, indicating that the model can localize lesions characterized by scorched margins and irregular spread.

Challenging recognition group: In contrast, white spot disease (whitespot) and algal leaf disease (algalleaf) show slightly lower detection accuracy, with AP values of 0.697 and 0.620, respectively. This is mainly because early white spot lesions are extremely small and often appear as pixel-level speckles, which can be confused with water stains or specular highlights on the tea leaf surface. In addition, the attached texture of algal leaf disease has substantial visual overlap with healthy leaf veins (Fig.9).

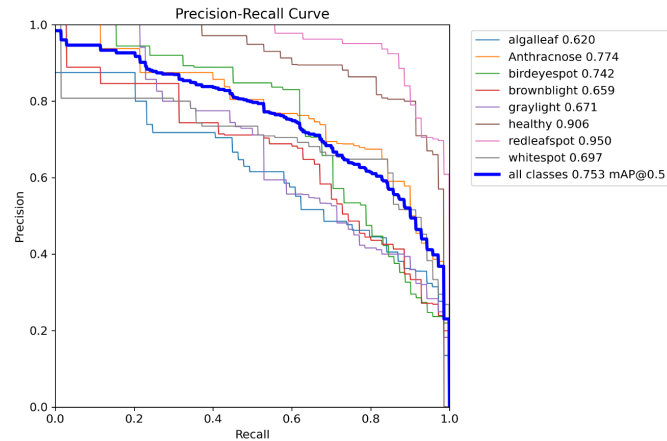


Fig. 9 Precision-Recall Curve of the Tea Leaf Disease Detection Model

4.3. Confusion Matrix and Feature Misclassification Analysis

To further examine the distribution of false positives (False Positives) and false negatives (False Negatives) in class prediction, this study uses a confusion matrix (Confusion Matrix) for cross-validation through combined qualitative and quantitative analysis (Fig.10).

The visualization of the confusion matrix clearly reflects the decision boundaries of the model. The results show that dark blocks along the diagonal, which represent correctly classified samples, are dominant, especially for the healthy and redleafspot categories, where the misclassification rate is very low.

However, the off-diagonal regions also reveal several misclassification patterns worthy of further analysis:

1) Background interference: Gray spot disease (graylight) is occasionally misclassified as the background environment (Background FN). This usually occurs under low illumination, where the color vectors of gray lesions are highly similar to those of soil or shadowed background regions.

2) Morphological confusion: A very small number of cross-class misclassifications occur between anthracnose (Anthracnose) and other morphologically similar large-area necrotic lesions. This suggests that certain fungal infections may exhibit macroscopically convergent visual appearances at specific stages of disease development.

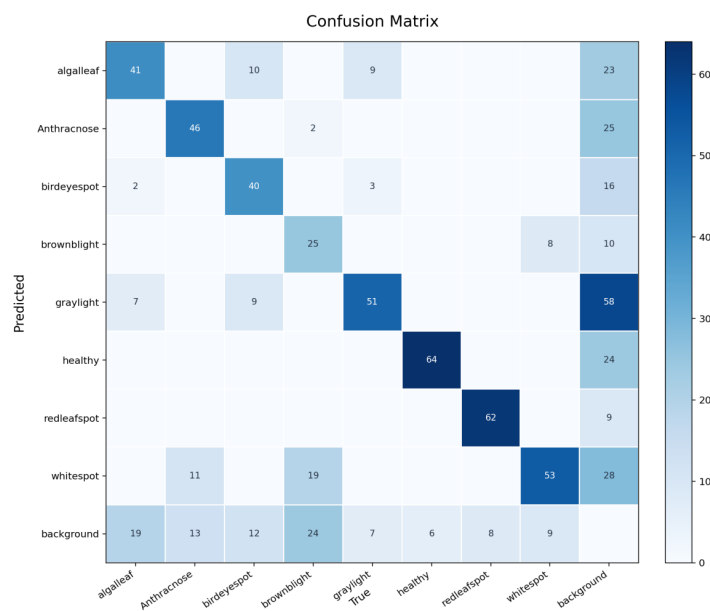


Fig. 10 Confusion Matrix Distribution for Multi-Class Tea Leaf Disease Detection on the Test Set

4.4. Real-Time Edge Inference and Deployment Efficiency

In practical smart tea plantation deployment, the computational complexity and inference speed of the algorithm directly determine whether the system can operate collaboratively with agricultural automation equipment, such as automatic spraying unmanned aerial vehicles or ground robots. In this study, the trained YOLOv10 model is exported in a lightweight form and deployed on the edge computing core of the customized handheld terminal, represented by the collaborative STM32 and Raspberry Pi architecture. Under stress testing in real environments, the system achieves an end-to-end inference speed of 150 FPS, benefiting from the architectural advantage of the NMS-free YOLOv10 design. This value substantially exceeds the real-time processing requirement of conventional video streams (30 FPS), indicating that the system can process highly concurrent image data with millisecond-level latency. This real-time performance provides sufficient computational margin and response time for subsequent closed-loop visual decision-making, such as variable-rate precision spraying control.

References

- [1] Wu H C. *Integrated Control Techniques for Brown Leaf Spot Disease of Tea* [J]. *Agriculture and Technology*, 2015(16). DOI:10.11974/myjjs.20150833093.
- [2] Wang K, Liu D M. *Intelligent Recognition Method for Tea Leaf States Based on Deep Learning* [J]. *Journal of Chongqing University of Technology (Natural Science)*, 2015(12). DOI:10.3969/j.issn.1674-8425(z).2015.12.020.
- [3] Chen L J, Xu B L. *Discussion on Approaches to Improving Tea Output Value* [J]. *Guizhou Agricultural Sciences*, 2008(3). DOI:10.3969/j.issn.1001-3601.2008.03.071.
- [4] Zou Y, Hu G G. *Tea Plucking and Management* [J]. *Anhui Agricultural Science Bulletin*, 2005, 11(1): 71. DOI:10.3969/j.issn.1007-7731.2005.01.061.
- [5] Wang A, Chen H, Liu L, Chen K, Lin Z, Han J, et al. *YOLOv10: Real-Time End-to-End Object Detection* [J]. *arXiv preprint arXiv:2405.14458*, 2024. DOI:10.48550/arXiv.2405.14458.
- [6] Guo L, Chen H B, Cui Z M, Lai Z H, Huang W L, Lin T L, et al. *GDE-YOLO: a robust and accurate method for real-time tea leaf disease detection in complex plantation environments* [J]. *Engineering Agriculture*, 2026, 13(4): 26668-26681. DOI:10.15302/J-FASE-2026669.
- [7] Sun Y G, Wu F, Zhou Q Y. *A deep learning detection algorithm for tea diseases* [J]. *Journal of Xinyang Normal University (Natural Science Edition)*, 2024, 37(2): 246-251.
- [8] Ayon R, Mubin A S, Hridoy A A G, Mojumdar M U, Chakraborty N R, Islam M. *Deep Learning for Tea Leaf Disease Detection: Comparing VGG16, Vision Transformer, EfficientNetB3, and Xception* [C]//2024 15th International Conference on Computing Communication and Networking Technologies (ICCCNT). IEEE, 2024: 1-6. DOI:10.1109/ICCCNT61001.2024.10726203.
- [9] Huang F, Liu F, Wang Y, Luo F. *Research Progress and Prospect on Computer Vision Technology Application in Tea Production* [J]. *Journal of Tea Science*, 2019, 39(1): 81-87. DOI:10.13305/j.cnki.jts.2019.01.009.
- [10] Chen J, Zhang D, Nanekaran Y A, Li D. *Identification of plant disease images via a CNN-based region proposal approach* [J]. *IET Image Processing*, 2020, 14(11): 2384-2393.
- [11] Ge Z, Liu S, Wang F, Li Z, Sun J. *YOLOX: Exceeding YOLO Series in 2021* [J]. *arXiv preprint arXiv:2107.08430*, 2021.
- [12] Wang Y X, Zhang Y, Yang C Y, et al. *Research Progress in Image Recognition Technologies for Crop Diseases Based on Deep Learning* [J]. *Acta Agriculturae Zhejiangensis*, 2019(4). DOI:10.3969/j.issn.1004-1524.2019.04.21.
- [13] Huang X Y, Li J, Jiang S. *Research on Rice Variety Recognition Technology Based on Computer Vision* [J]. *Journal of Jiangsu University (Natural Science Edition)*, 2004(2). DOI:10.3969/j.issn.1671-7775.2004.02.003.
- [14] Long D F, Fan S C. *Application of Computer Vision to Log Volume Measurement* [J]. *Chinese Journal of Scientific Instrument*, 2004(z1). DOI:10.3321/j.issn:0254-3087.2004.z1.432.
- [15] Lan J H, Wang D, Shen X P. *Research Progress of Convolutional Neural Networks in Visual Image Detection* [J]. *Chinese Journal of Scientific Instrument*, 2020(4). DOI:10.19650/j.cnki.cjsi.J2006003.
- [16] Sun X X. *The Research of Tea Buds Detection and Leaf Diseases Image Recognition Based on Deep Learning* [D]. Tai'an: Shandong Agricultural University, 2019.
- [17] Chen M T. *Recognition and Location of High-Quality Tea Buds Based on Computer Vision* [D]. Qingdao: Qingdao University of Science and Technology, 2019.